Bioorganic & Medicinal Chemistry 18 (2010) 7022–7028

Contents lists available at ScienceDirect

Bioorganic & Medicinal Chemistry

journal homepage: www.elsevier.com/locate/bmc

Retinobenzaldehydes as proper-trafficking inducers of folding-defective P23H rhodopsin mutant responsible for *Retinitis Pigmentosa*

Kenji Ohgane [a,*], Kosuke Dodo [b], Yuichi Hashimoto [a]

[a] Institute of Molecular and Cellular Biosciences, The University of Tokyo, 1-1-1, Bunkyo-ku, Tokyo 113-0032, Japan
[b] RIKEN, Advanced Science Institute (ASI), 2-1 Hirosawa, Wako, Saitama 351-0198, Japan

ARTICLE INFO

Article history:
Received 15 July 2010
Revised 4 August 2010
Accepted 5 August 2010
Available online 11 August 2010

Keywords:
Rhodopsin
Trafficking
Retinitis pigmentosa
Retinobenzaldehyde
Mutant

ABSTRACT

The *Retinitis* pigmentosa (RP)-causing mutant of rhodopsin, P23H rhodopsin, is folding-defective and unable to traffic beyond the endoplasmic reticulum (ER). This ER retention, and in some cases aggregation, are proposed to result in ER-stress and eventually cell death. The endogenous rhodopsin ligand 11-*cis*-retinal and its isomer 9-*cis*-retinal have been shown to act as pharmacological chaperones, promoting proper folding and trafficking of the P23H rhodopsin. In spite of this promising effect, the development of retinals and related polyenealdehydes as pharmacological agents has been hampered by their undesirable properties, which include chemical instability, photolability, and potential retinoidal actions. Here, we report the design and synthesis of a class of more stable nonpolyene-type rhodopsin ligands, structurally distinct from, and with lower toxicity than, retinals. A structure–activity relationship study was conducted using cell-surface expression assay to quantify folding/trafficking efficiency of P23H rhodopsin.

1. Introduction

Retinitis pigmentosa (RP) comprises a heterogeneous group of inherited retinal disorders that lead to photoreceptor death, resulting in night blindness and loss of central vision; no therapy is currently available.[1–4] Nearly 50% of patients with autosomal dominant RP (ADRP) have a mutation in rhodopsin, with the first-reported and the most frequent mutation being Pro23His (P23H); this mutation accounts for approximately one-third of RP-causing rhodopsin mutations.[4,5] The P23H mutant, unlike wild-type (WT) rhodopsin, has been considered to be folding-defective (misfolded), and as a result, it forms the pigment poorly, does not acquire the Golgi-related glycosylation, and is retained within the cell on endoplasmic reticulum (ER).[6–8] The ER-retained mutants are considered to form toxic aggregates, causing ER-stress and impairment of the ubiquitin-proteasome system, which result in photoreceptor cell death.[9–11]

Thus, the folding-defective nature, linked to abnormal trafficking (retention in ER), of P23H rhodopsin mutant lies at the center of the etiology of ADRP, at least in part.[12–14] If the P23H mutant can be induced to fold properly, this might lead to recovery of normal trafficking of the mutant rhodopsin, providing a promising strategy for treatment of the corresponding ADRP. One possible approach would be application of so-called pharmacological chaperones, small molecules that facilitate folding and trafficking of folding-defective proteins, presumably by binding to the folding intermediate in the ER.[15–18] Noorwez et al. reported that retinals, including the endogenous rhodopsin ligand 11-*cis*-retinal and its isomer 9-*cis*-retinal (Fig. 1A), as well as some 11-*cis*-locked analogues, act as pharmacological chaperones and promote proper folding of P23H rhodopsin mutant, consequently promoting trafficking of the ER-retained mutant to the plasma membrane.[19–22] The in vivo effectiveness of this strategy is supported by the fact that supplementation of vitamin A, the precursor of 11-*cis*-retinal, slowed the rate of photoreceptor degeneration in model mice harboring T17M rhodopsin mutant.[23] Although the potential therapeutic benefit of retinals (and the precursor, vitamin A) has been recognized, the chemical instability and photolability of retinals, and the potential retinoidal actions of their metabolites, such as retinoic acid, are problematic, especially for clinical application. To overcome these problems, we started structural development studies to create stable ligands, which are structurally distinct from retinals and/or polyene aldehydes, for P23H rhodopsin mutant.

2. Results and discussion

2.1. Cell-surface expression assay

For structural development studies of P23H rhodopsin ligands which would induce folding and cell-surface trafficking of the protein, establishment of a quantitative assay system is mandatory. We selected a cell-based assay system, using HEK293 cells transiently expressing N-terminally hemaglutinin (HA)-tagged

* Corresponding author. Tel.: +81 3 5841 7848; fax: +81 3 5841 8495.
E-mail address: zbg04414.park@orange.zero.jp (K. Ohgane).

0968-0896/$ - see front matter © 2010 Elsevier Ltd. All rights reserved.
doi:10.1016/j.bmc.2010.08.014

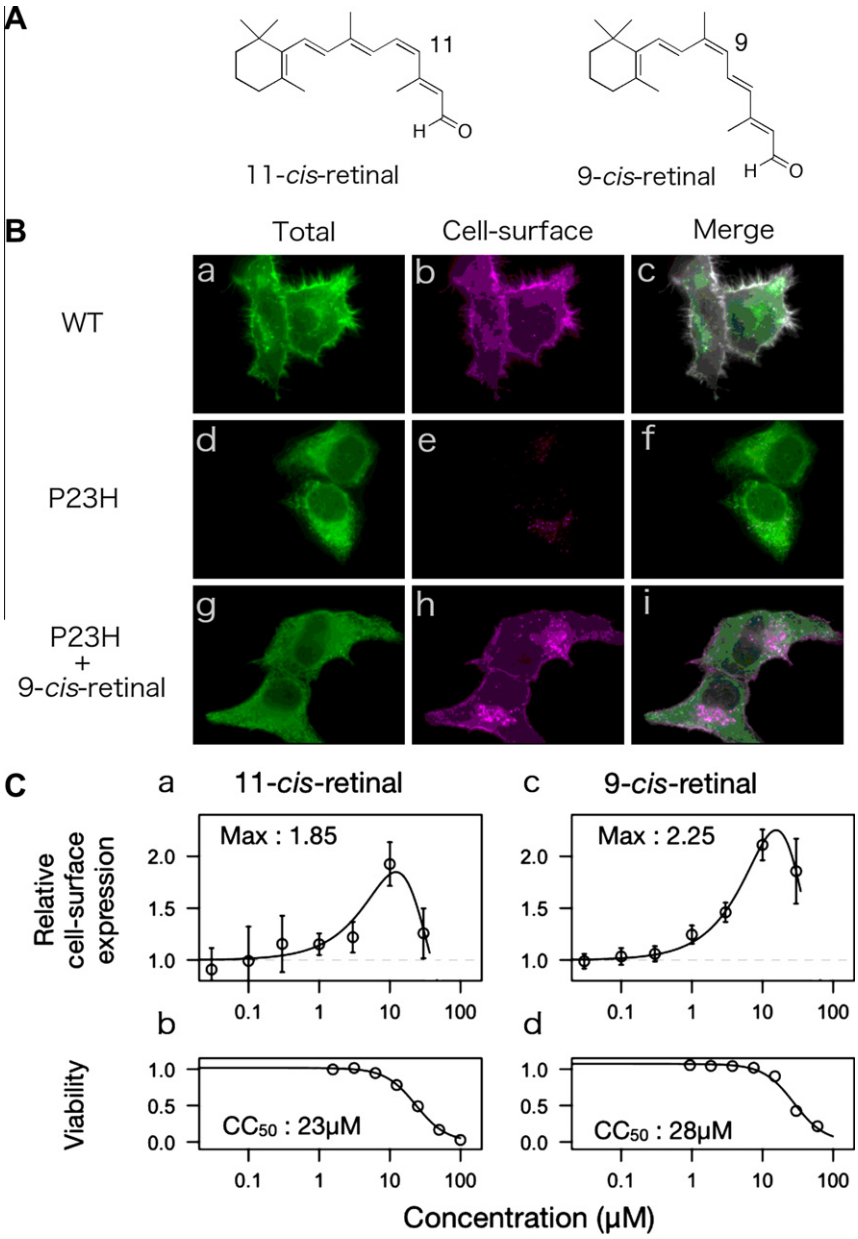

Figure 1. Subcellular localization of P23H mutant and dose-dependent, retinal-induced translocation of the mutant to the plasma membrane. (A) Structures of 11-*cis*-retinal and 9-*cis*-retinal. (B) Subcellular localization of HA-tagged rhodopsin (WT and P23H) in HEK293 cells was examined by immunofluorescence microscopy. HEK293 cells were transiently transfected with HA-tagged human rhodopsin (WT or P23H mutant), and incubated for 22 h in the presence or absence of 15 μM 9-*cis*-retinal. Before fixation, cells were incubated with anti-HA antibody for 1 h and then fixed, permeabilized, and blocked. Then, cells were incubated with anti-rhodopsin antibody and processed for immunofluorescence microscopy. FITC- or TRITC-labeled secondary antibody was used for anti-rhodopsin or anti-HA, respectively. (C) The effect of the retinals on the cell-surface expression level of the P23H mutant was evaluated by cell-surface ELISA of non-permeabilized cells with anti-HA. Both of the retinals dose-dependently enhanced the cell-surface trafficking of the mutant, although significant toxicity was observed at higher concentrations. The graphs represent the average values of at least two independent experiments (n >4), and the error bars represents 95% confidence intervals. The lower panels show viability of cells exposed to the retinals, evaluated using a water-soluble tetrazolium, WST-1.

wild-type (WT) or P23H rhodopsin (see Section 4). To analyze the localization of WT or P23H rhodopsin, HA-tagged rhodopsins were immunostained under cell membrane-permeabilized and non-permeabilized conditions (Fig. 1B), that is, all the expressed rhodopsin was detected with anti-rhodopsin antibody under the permeabilized condition (Fig. 1B, panels a, d, and g), whereas only the rhodopsin trafficked to the cell surface could be detected with anti-HA antibody under the non-permeabilized condition (Fig. 1B, panels b, e, and h) (see Section 4). As shown in Figure 1B, WT rhodopsin was confirmed to be mainly localized at the cell surface (Fig. 1B, panels b), and P23H mutant rhodopsin showed a perinuclear/reticular distribution characteristic of ER retention (Fig. 1B, panel d), with almost no expression on the cell surface (Fig. 1B, panel e), as confirmed by colocalization with ER marker PDI. All of these results are in accordance with previous findings.[6,11,19,20] When P23H rhodopsin-expressing cells were cultured in the presence of 11-*cis*-retinal or 9-*cis*-retinal (Fig. 1A), a substantial portion of the P23H rhodopsin was trafficked to the cell surface (Fig. 1B, panel h). Thus, the cell-surface expression level of the P23H mutant can be regarded as reflecting its folding/trafficking efficiency, and seems to be a direct measure of the potency of 11-*cis*-retinal or 9-*cis*-retinal as a pharmacological chaperone. To quantitatively

evaluate the cell-surface expression level, we conducted Cell-ELISA under a non-permeabilized condition (Fig. 1C, panels a and c, vertical scale: relative amount of P23H rhodopsin expressed on the cell surface when that of non-treated cells is defined as 1.0).[24] This quantification method allowed us to measure the total amount of P23H mutant rhodopsin expressed on the cell surface in one well. As shown in Figure 1C (panels a and c), both 11-*cis*- and 9-*cis*-retinal induced cell membrane trafficking of P23H rhodopsin dose-dependently in the concentration range of 0.1–10 μM. At the same time, the cytotoxicity of these compounds was evaluated with WST-1, a water-soluble tetrazolium (Fig. 1C, panels b and d) (see Section 4). The 50% cytotoxic concentration (CC_{50}) values of 11-*cis*- and 9-*cis*-retinal were determined to be 23 and 28 μM, respectively, both of which are within the concentration range used for cell-surface P23H rhodopsin quantification. As a result, the dose–response curves of cell-surface P23H rhodopsin expression were bell-shaped for both 11-*cis*- (Fig. 1C, panel a) and 9-*cis*-retinal (Fig. 1C, panel b), because of their cytotoxicity as shown in the figures. This assay system is intrinsically reproducible, and we adopted this method for our structural development study described below.

2.2. Molecular design

2.2.1. Discovery of lead compound

Our previous investigations concerning synthetic retinoids, that is, structural development studies of all-*trans*-retinoid acid (ATRA, Fig. 2A), resulted in creation of a group of active compounds named retinobenzoic acids, including Am80 (tamibarotene), Am555S (TAC-101) and Ch55 (Fig. 2A).[25–28] The results suggested that the triene carboxylic acid moiety and the cyclohexenylethylene moiety of ATRA can be substituted with a benzoic acid moiety and a tetrahydrotetramethylnaphthalenyl (TM) moiety, respectively. Therefore, we expected that hybrid compounds bearing a benzaldehyde moiety and TM moiety would be active analogs of 11-*cis*- and/or 9-*cis*-retinal. Based on this strategy, we first designed retinobenzal-

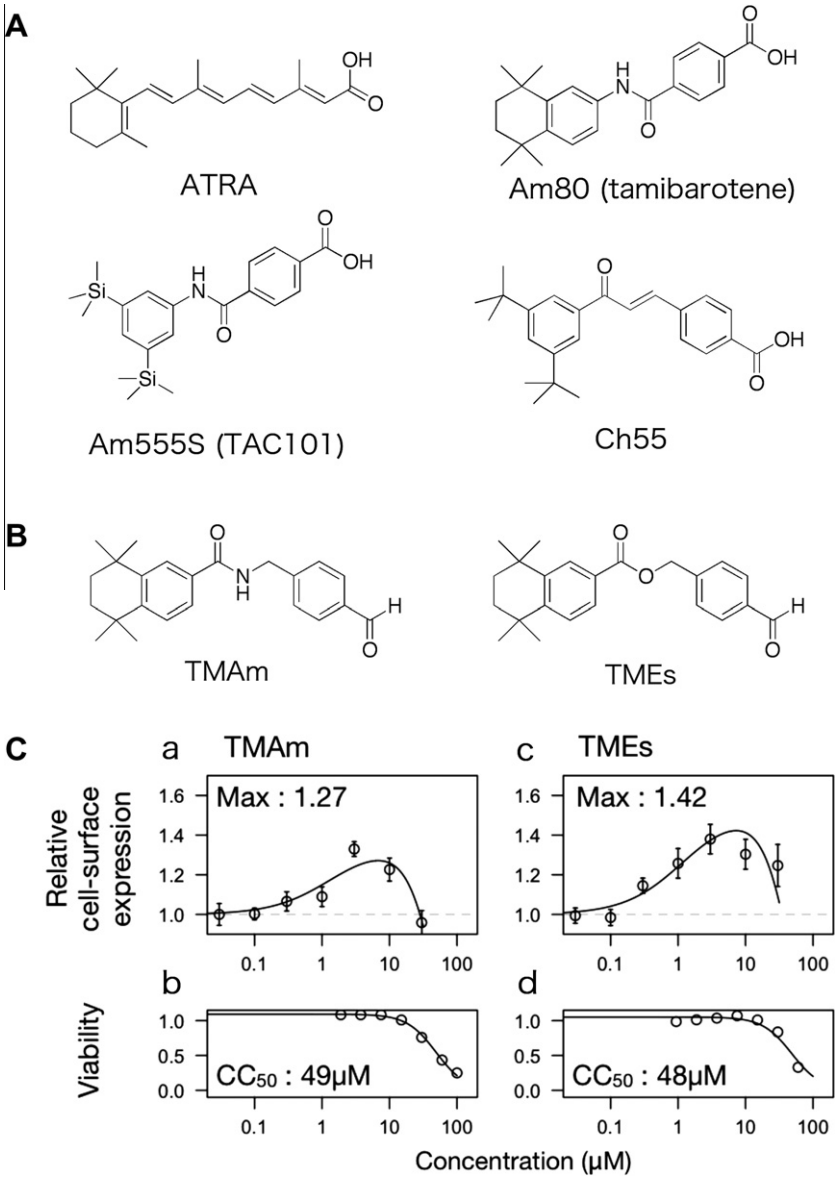

Figure 2. Molecular design of retinobenzaldehydes, TMAm/TMEs. (A) Structures of ATRA and retinobenzoic acids. (B) Structures of TMAm and TMEs. (C) Effect of TMAm and TMEs on cell surface expression level of P23H mutant rhodopsin. The graphs show the average values of at least three independent experiments (n >6), and each error bar represents the standard error of the mean.

dehydes, TMAm and TMEs, which possess the same hydrophobic TM moiety as Am80, together with a benzaldehyde moiety, with the linker being changed to mimic the conformation of 11-*cis*-retinal (Fig. 2B). TMAm and TMEs were prepared by usual organic synthetic methods. Briefly, 5,6,7,8-tetrahydro-5,5,8,8-tetramethylnaphthalene-2-carboxylic acid[29] was converted to acyl chloride with oxalyl chloride, and then condensed with 4-hydroxymethylbenzylamine to give *N*-(4-(hydroxymethyl)benzyl)-5,6,7,8-tetrahydro-5,5,8,8-tetramethylnaphthalene-2-carboxamide, which was oxidized with manganese dioxide in dichloromethane to give TMAm. TMEs was prepared by condensation of 5,6,7,8-tetrahydro-5,5,8,8-tetramethylnaphthalene-2-carboxylic acid with *p*-xylene-α,α′-diol, followed by oxidation.

As shown in Figure 2C (panels a and c), both of the designed compounds, TMAm and TMEs, enhanced the cell-surface expression of P23H rhodopsin in a dose-dependent manner, though the efficacy was lower than that of 11-*cis*- or 9-*cis*-retinal. However, both TMAm and TMEs were less cytotoxic than retinals (Fig. 2C, panels b and d). Moreover, these compounds have the advantage that their basic architectures are structurally distinct from retinals, and they are more stable than 11-*cis*-retinal, which readily isomerizes to the all-*trans* isomer on brief exposure to visible light. Of these two retinobenzaldehydes, TMEs seemed to be superior in its efficacy to induce P23H rhodopsin-trafficking to the cell surface. Therefore, we selected TMEs as a lead compound for further structural development study.

2.2.2. Structure–activity relationship of the hydrophobic part

As mentioned above, we regarded the TM moiety of TMAm/TMEs as a structural mimic of the ionone-like head group (1-butenyl-2,6,6-trimethyl-2-cyclohexene) moiety of 11-*cis*-/9-*cis*-retinal. To assess the contribution of the four methyl groups on the TM moiety of TMEs, we designed HNEs (the derivative lacking the four methyl groups), TB4Es and TB3Es (Fig. 3A). All the compounds were prepared by methods similar to that used for the preparation of TMEs.

The removal of all four methyl groups of the TM moiety, that is, HNEs, resulted in loss of the trafficking-promoting activity, indicating an important role of the methyl groups in the interaction within the binding site of P23H mutant rhodopsin (Fig. 3B, panel a). This result is consistent with previous reports that 11-*cis*-retinal analogues lacking their ring methyl groups show no or significantly reduced binding to rhodopsin,[30,31] and is also consistent with the view that the binding site of our compounds is the same as that of 11-*cis*-retinal. Concerning the analogs retaining a half of the tetramethylcyclohexane skeleton in the TM moiety, that is, TB4Es and TB3Es, the former (the *para*-analog) shows no enhancement of P23H rhodopsin-trafficking (Fig. 3B, panel b), and only the *meta*-analog TB3Es enhanced cell-surface expression of the mutant with comparable efficacy to that of TMEs (Fig. 3B, panel c). The results suggested a greater contribution of the methyl groups at the 3-position.

In the case of synthetic retinoids, the 3,5-disubsituted phenyl moiety has been quite useful as a structural substitute for TM structure, as found in Am555S (TAC-101) and Ch55 (Fig. 2A).[25,26] This led us design and prepare a 3,5-di-*tert*-butyl derivative, TB35Es (Fig. 3A). The hydrophobic pocket of the receptor(s) of retinoids, that is, nuclear retinoic acid receptors (RARs), seems to be sufficiently large/wide that the site can accommodate a large hydrophobic group, even a diadamantyl-substituted phenyl group,[32–34] though this compound is an antagonist. The corresponding hydrophobic pocket of rhodopsin appears to be smaller than that of RARs, as estimated from the reported X-ray structure of rhodopsin.[35,36] Therefore, we also designed and prepared a smaller 3,5-bis-trifluoromethyl derivative, CF35Es (Fig. 3A). These compounds were also prepared by methods similar to that used for the preparation of TMEs.

TB35Es showed P23H mutant rhodopsin-trafficking-inducing activity and cytotoxicity with almost the same potency as TMEs (Fig. 3B: panel d, and Fig. 2C: panels c and d). The bis-trifluoromethyl analog, CF35Es, showed the most potent P23H rhodopsin-trafficking-inducing activity among the compounds we prepared (Fig. 3B, panel e). Its efficacy is comparable to that of 11-*cis*-retinal (Fig. 1C, panel a). In addition, greatly reduced cytotoxicity was observed for CF35Es. That is, this compound is one of the least cytotoxic among the P23H rhodopsin-trafficking-inducing activity-positive compounds, including 11-*cis*-/9-*cis*-retinal and TMEs. Therefore, CF35Es should be a superior lead compound for the development of pharmacological chaperones for the treatment of RP.

2.2.3. Bioisoster of aldehyde group

From the viewpoint of clinical application, the aldehyde group of retinobenzaldehyde (which is expected to form a covalent Schiff base with rhodopsin) might be better exchanged to a non-Schiff base-forming bioisoster. The side chain amino group of Lys296 is

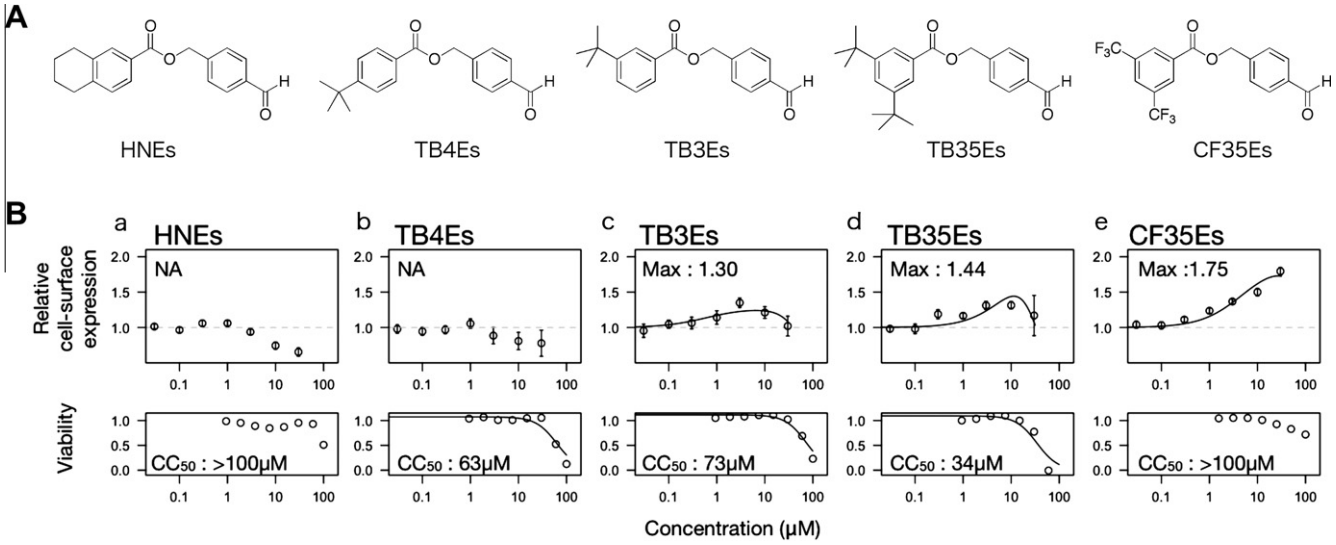

Figure 3. Retinobenzaldehydes. (A) Structures of retinobenzaldehydes. (B) Effects of retinobenzaldehydes on cell-surface expression level of P23H mutant rhodopsin.

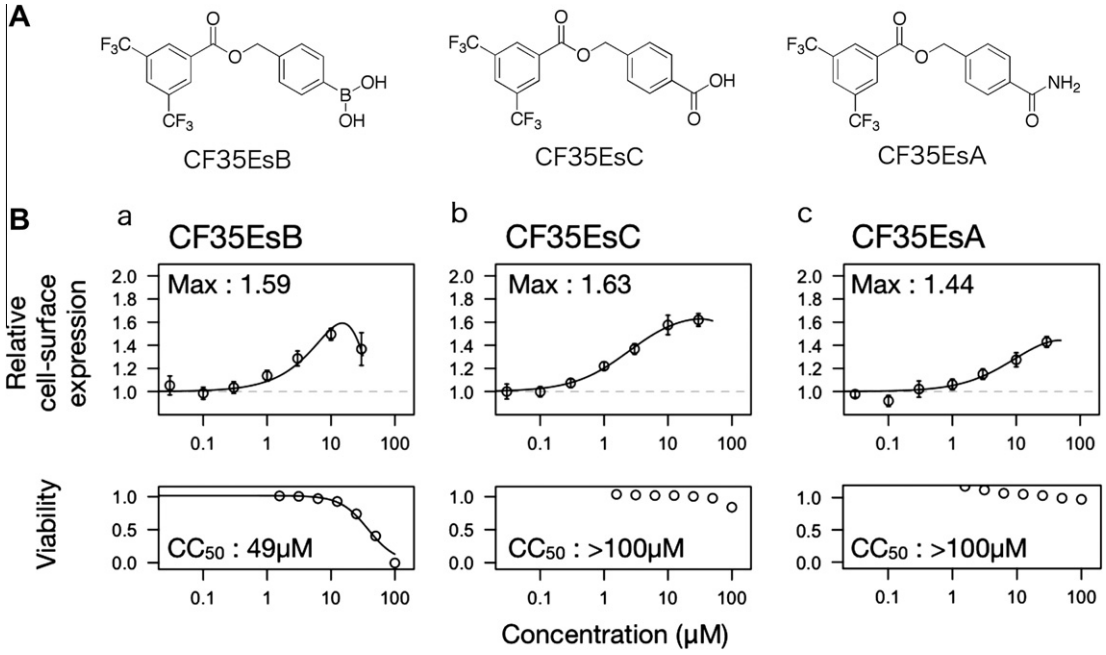

Figure 4. Retinobenzaldehyde analogs. (A) Structures of retinobenzaldehyde analogs. (B) Effects of retinobenzaldehyde analogs on cell surface expression level of P23H mutant rhodopsin.

involved in the covalent interaction.[37] As alternative functional groups, which are expected to possess affinity for the amino group, we selected boronic acid (anticipating electronic interaction and coordination of a lone pair of the amino group to the boron atom), carboxylic acid (electronic interaction), and primary amide (as a hydrogen bond-forming functionality). Thus, CF35EsB, CF35EsC, and CF35EsA were designed and prepared (Fig. 4A).

As expected, all of the compounds thus designed showed moderate to potent P23H rhodopsin-trafficking-inducing activity (Fig. 4B), though the methyl ester of CF35EsC completely lost activity, implying the importance of the acidic proton(s). Although CF35EsB showed similar cytotoxicity to that elicited by 11-*cis*-/9-*cis*-retinal, the other two derivatives, CF35EsC and CF35EsA, showed very weak cytotoxicity, resembling CF35Es in that respect.

3. Conclusion

We have developed retinobenzaldehydes and their analogs that induce proper trafficking of P23H rhodopsin, using the same strategy adopted for our previous synthetic retinoid studies together with cell-surface expression assay of the mutant. As a result, superior folding/trafficking inducers of P23H mutant rhodopsin with low cytotoxicity, including CF35Es and CF35EsC, were obtained. These compounds should be superior lead compounds for the development of pharmacological chaperones for the treatment of ADRP. Studies are in progress to examine in detail the molecular mechanism(s) of P23H rhodopsin-trafficking-induction, and the effects of these compounds on other rhodopsin mutants.

4. Experimental

4.1. Materials for biological studies

The expression plasmid of WT rhodopsin was purchased from GeneCopoeia. Primers for PCR and inverse PCR was obtained from Invitrogen. PCR was carried out on a Gene Amp PCR System 9700 (Perkin Elmer).

4.2. Site-directed mutagenesis

WT and P23H rhodopsin tagged at the N-terminal end with the HA epitope (YPYDVPDYA) were generated by inverse PCR mutagenesis with the KOD-plus-, Ligation High, and T4 polynucleotide kinase (Toyobo Co., Ltd). The constructs were confirmed by DNA sequencing.

4.3. Cell culture and transfection

HEK293 cells were grown in Dulbecco's modified Eagle's medium (DMEM) supplemented with 5% fetal bovine serum and penicillin and streptomycin at 37 °C in a humidified 5% CO_2 incubator. Cells were transfected by a calcium phosphate precipitation.

4.4. Immunofluorescence microscopy

For dual labeling of cell surface (anti-HA) and total (anti-rhodopsin 1D4) rhodopsin, HEK293 cells were seeded into poly-lysine (from Chemicon) coated glass-based dishes (1×10^5 cells/dish, from Iwaki) 20 h prior to transfection. At 2 h after transfection, the cells were incubated with 1:1000 dilution of rabbit anti-HA antibody (A190-108A; Bethyl Laboratories, Inc.) in OptiMEM for 1 h at 37 °C, then washed three times with PBS containing 0.1% BSA, fixed (4% formaldehyde in PBS, 30 min, rt), permeabilized (0.1% Triton X in PBS, 10 min, rt), and blocked (1% BSA + 0.05% tween 20 in PBS, 1 h, rt). Then the cells were incubated with 1:400 dilution of anti-rhodopsin (1D4, MAB5356; Chemicon) for 1 h, followed by incubation with secondary antibody (1:500 dilution of FITC-conjugated anti-mouse antibody and 1:800 dilution of TRITC-conjugated anti-rabbit antibody). All images were obtained using an Olympus IX70 fluorescence microscope.

4.5. Cell-surface ELISA

HEK293 cells were seeded into poly-lysine-coated 96-well plates (1×10^4 cells/well), and transfected after 16–20 h. Then, 2–3 h later, the cells were treated with prediluted compounds in

DMEM containing 5% FBS (DMSO final concentration; 0.1%). After 20 h incubation, the cells were fixed, blocked as described above and incubated with a 1:7000 dilution of HRP-conjugated anti-HA polyclonal antibody (A190-108P; Bethyl Laboratories, Inc., CanGet-Signal immunoreaction enhancer solution; Toyobo Co., Ltd) for 1.5 h at room temperature. After extensive washing of the cells with PBS containing 0.05% Tween 20, 50 μL of chemiluminescent HRP substrate (SuperSignal ELISA Pico chemiluminescent substrate; Pierce Biotechnology, Inc.) was added. After shaking at room temperature for 10 min, the chemiluminescence was measured with a Perkin Elmer Wallac 1420 multilabel counter. The relative luminescence was defined as (compound-treated well − average of background wells)/(average of vehicle-treated wells − average of background wells).

4.6. WST-1 viability assay

HEK293 cells were seeded into poly-Lys-coated 96-well plates (1×10^4 cells/well), and incubated for 16–20 h. The cells were then treated with prediluted compounds in DMEM containing 5% FBS (DMSO final concentration; 0.1%). After 20–22 h incubation, 10 μL of WST-1 reagent (WST-1 5 mM, 1-methoxy-5-methylphenazinium methylsulfate 100 mM, HEPES 20 mM, pH 7.4) were added. After 2 h incubation the absorbance was read at 405 nm using a Perkin Elmer Wallac 1420 multilabel counter. The viability was defined as Abs_{405} (treated)/Abs_{405} (vehicle) after subtraction of background absorbance (from wells without cells). WST-1 reagent was purchased from Dojindo.

4.7. *N*-(4-Formylbenzyl)-5,6,7,8-tetrahydro-5,5,8,8-tetramethylnaphthalene-2-carboxamide (TMAm)

^{1}H NMR ($CDCl_3$): δ 10.00 (s, 1H), 7.86 (d, J = 8.0 Hz, 2H), 7.83 (d, J = 1.8 Hz, 1H), 7.52 (d, J = 8.0 Hz, 2H), 7.49 (dd, J = 8.3, 1.8 Hz, 1H), 7.37 (d, J = 8.32 Hz, 1H), 6.49 (br s, 1H), 4.74 (d, J = 6.1 Hz, 2H), 1.70 (s, 4H), 1.31 (s, 6H), 1.29 (s, 6H); MS (FAB): m/z 350 $(M+H)^+$; HR-MS calcd for $C_{23}H_{28}NO_2$ $(M+H)^+$: 350.2120. Found 350.2095; mp: 158–160 °C.

4.8. 4-Formylbenzyl 5,6,7,8-tetrahydro-5,5,8,8-tetramethylnaphthalene-2-carboxylate (TMEs)

^{1}H NMR ($CDCl_3$): δ 10.03 (s, 1H), 8.05 (d, J = 1.8 Hz, 1H), 7.90 (d, J = 8.5 Hz, 2H), 7.82 (dd, J = 8.5, 1.8 Hz, 1H), 7.59 (d, J = 7.9 Hz, 2H), 7.39 (d, J = 7.9 Hz, 1H), 5.43 (s, 2H), 1.70 (s, 4H), 1.31 (s, 6H), 1.30 (6H); MS (FAB): m/z351 $(M+H)^+$; HR-MS calcd for $C_{23}H_{27}O_3$ (M+H): 351.1960. Found 351.1966.

4.9. 4-Formylbenzyl 5,6,7,8-tetrahydronaphthalene-2-carboxylate (HNEs)

^{1}H NMR ($CDCl_3$): δ 10.03 (1H, s), 7.90 (2H, d, J = 7.9 Hz), 7.79 (1H, s), 7.79 (1H, d, J = 8.5 Hz), 7.59 (2H, d, J = 7.9 Hz), 7.14 (1H, d, J = 8.5 Hz), 5.42 (2H, s), 2.82 (4H, br s), 1.84–1.80 (4H, br m); MS (FAB): m/z 295 $(M+H)^+$; HR-MS calcd for $C_{19}H_{19}O_3$ $(M+H)^+$: 295.1334. Found 295.1368.

4.10. 4-Formylbenzyl 3-*tert*-butylbenzoate (TB3Es)

^{1}H NMR ($CDCl_3$): δ 10.03 (1H, s), 8.13 (1H, t, J = 2.1 Hz), 7.92–7.90 (3H, m), 7.63–7.61 (3H, m), 7.40 (1H, t, J = 7.6 Hz), 5.45 (2H, s), 1.35 (9H, s); MS (FAB): m/z 297 $(M+H)^+$, 295 $(M-H)^+$; HR-MS calcd for $C_{19}H_{21}O_3$ $(M+H)^+$: 297.1491. Found 297.1462; mp: 53–55 °C.

4.11. TB4Es: 4-formylbenzyl 4-*tert*-butylbenzoate (TB4Es)

^{1}H NMR ($CDCl_3$): δ 10.03 (1H, s), 8.03 (2H, d, J = 8.5 Hz), 7.90 (2H, d, J = 8.5 Hz), 7.60 (2H, d, J = 8.5 Hz), 7.48 (2H, d, J = 8.5 Hz), 5.44 (2H, s), 1.34 (9H, s); MS (FAB): m/z 297 $(M+H)^+$; HR-MS calcd for $C_{19}H_{21}O_3$ $(M+H)^+$: 297.1491. Found 297.1496; mp: 33–35 °C.

4.12. TB35Es: 4-formylbenzyl 3,5-di-*tert*-butylbenzoate (TB35Es)

^{1}H NMR ($CDCl_3$): δ 10.03 (1H, s), 7.94 (2H, d, J = 1.8 Hz), 7.91 (2H, d, J = 7.9 Hz), 7.66 (1H, t, J = 1.8 Hz), 7.61 (2H, d, J = 7.9 Hz), 5.46 (2H, s), 1.35 (18H, s); MS (FAB): m/z 353 $(M+H)^+$, 351 $(M-H)^+$; HR-MS calcd for $C_{23}H_{29}O_3$ $(M+H)^+$: 353.2117. Found 353.2147; mp: 51–53 °C.

4.13. CF35Es: 4-formylbenzyl 3,5-bis(trifluoromethyl)benzoate (CF35Es)

^{1}H NMR ($CDCl_3$): δ 10.05 (1H, s), 8.52 (2H, s), 8.09 (1H, s), 7.94 (2H, d, J = 7.9 Hz), 7.62 (2H, d, J = 7.9 Hz), 5.51 (2H, s); MS (FAB): m/z 377 $(M+H)^+$, 375 $(M-H)^+$; HR-MS calcd for $C_{17}H_{11}F_6O_3$ (M+H): 377.0612. Found 377.0652. Calcd for $C_{17}H_9F_6O_3$ (M−H): 375.0456. Found 375.0473; mp: 83–85 °C.

4.14. CF35EsB: 4-((3,5-bis(trifluoromethyl)benzoyloxy)methyl)-phenylboronic acid (CF35EsB)

^{1}H NMR ($CDCl_3$): δ 8.50 (2H, s), 8.07 (1H, s), 7.80 (2H, d, J = 7.9 Hz), 7.50 (2H, d, J = 7.9 Hz), 5.46 (2H, s); mp: 194–197 °C.

4.15. CF35EsC: 4-((3,5-bis(trifluoromethyl)benzoyloxy)methyl)-benzoic acid (CF35EsC)

^{1}H NMR ($CDCl_3$): δ 8.52 (2H, s), 8.14 (2H, d, J = 7.9 Hz), 8.09 (1H, s), 7.56 (2H, d, J = 7.9 Hz), 5.50 (2H, s); HR-MS calcd for $C_{17}H_{11}F_6O_3$ (M+H): 393.0561. Found 393.0538; mp: 160–163 °C.

4.16. CF35EsA: 4-carbamoylbenzyl 3,5-bis(trifluoromethyl)-benzoate (CF35EsA)

^{1}H NMR ($CDCl_3$): δ 8.51 (2H, s), 8.09 (1H, s), 7.87 (2H, d, J = 8.0 Hz), 7.55 (2H, d, J = 8.0 Hz), 6.06 (1H, br s), 5.60 (1H, br s), 5.48 (2H, s); HR-MS Calcd for $C_{17}H_{11}F_6O_3$ (M+H): 392.0721. Found 392.0568; mp: 169–172 °C.

Acknowledgments

The work described in this paper was partially supported by Grants-in-Aid for Scientific Research from The Ministry of Education, Culture, Sports, Science and Technology, Japan, and the Japan Society for the Promotion of Science.

References and notes

1. Rattner, A.; Sun, H.; Nathans, J. *Annu. Rev. Genet.* **1999**, *33*, 89.
2. Chapple, J. P.; Grayson, C.; Hardcastle, A. J.; Saliba, R. S.; van der Spuy, J.; Cheetham, M. E. *Trends Mol. Med.* **2001**, *7*, 414.
3. Kennan, A.; Aherne, A.; Humphries, P. *Trends Genet.* **2005**, *21*, 103.
4. Hartong, D.; Berson, E. L.; Dryja, T. P. *Lancet* **2006**, *368*, 1795.
5. Dryja, T. P.; McGee, T. L.; Reichel, E.; Hahn, L. B.; Cowley, G. S.; Yandell, D. W.; Sandberg, M. A.; Berson, E. L. *Nature* **1990**, *343*, 364.
6. Sung, C. H.; Schneider, B. G.; Agarwal, N.; Papermaster, D. S.; Nathans, J. *Proc. Natl. Acad. Sci. U.S.A.* **1991**, *88*, 8840.
7. Sung, C. H.; Davenport, C. M.; Nathans, J. *J. Biol. Chem.* **1993**, *268*, 26645.
8. Kaushal, S.; Khorana, H. G. *Biochemistry* **1994**, *33*, 6121.
9. Illing, M. E.; Rajan, R. S.; Bence, N. F.; Kopito, R. R. *J. Biol. Chem.* **2002**, *277*, 34150.
10. Mendes, H. F.; Cheetham, M. E. *Human Mol. Genet.* **2008**, *17*, 3043.

11. Saliba, R. S.; Munro, P. M.; Luthert, P. J.; Cheetham, M. E. *J. Cell Sci.* **2002**, *115*, 2907.
12. Mendes, H. F.; van der Spuy, J.; Chapple, J. P.; Cheetham, M. E. *Trends Mol. Med.* **2005**, *11*, 177.
13. Lem, J.; Krasnoperova, N. V.; Calvert, P. D.; Kosaras, B.; Cameron, D. A.; Nicolò, M.; Makino, C. L.; Sidman, R. L. *Proc. Natl. Acad. Sci.* **1999**, *96*, 736.
14. Humphries, M. M.; Rancourt, D.; Farrar, G. J.; Kenna, P.; Hazel, M.; Bush, R. A.; Sieving, P. A.; Sheils, D. M.; McNally, N.; Creighton, P.; Erven, A.; Boros, A.; Gulya, K.; Capecchi, M. R.; Humphries, P. *Nat. Genet.* **1997**, *15*, 216.
15. Loo, T. W.; Clarke, D. M. *J. Biol. Chem.* **1997**, *272*, 709.
16. Morello, J. P.; Salahpour, A.; Laperriere, A.; Bernier, V.; Arthus, M.-F.; Lonergan, M.; Petaja-Repo, U.; Angers, S.; Morin, D.; Bichet, D. G.; Bouvier, M. *J. Clin. Invest.* **2000**, *105*, 887.
17. Morello, J. P.; Petaja-Repo, U. E.; Bichet, D. G.; Bouvier, M. *Trends Pharmacol. Sci.* **2000**, *21*, 466.
18. Ishii, S.; Kase, R.; Sakuraba, H.; Suzuki, Y. *Biochem. Biophys. Res. Commun.* **1993**, *197*, 1585.
19. Noorwez, S. M.; Kuksa, V.; Imanishi, Y.; Zhu, L.; Filipek, S.; Palczewski, K.; Kaushal, S. *J. Biol. Chem.* **2003**, *278*, 14442.
20. Noorwez, S. M.; Malhotra, R.; McDowell, J. H.; Smith, K. A.; Krebs, M. P.; Kaushal, S. *J. Biol. Chem.* **2004**, *279*, 16278.
21. Noorwez, S. M.; Ostrov, D. A.; McDowell, J. H.; Krebs, M. P.; Kaushal, S. *Invest. Ophtthalmol. Visual Sci.* **2008**, *49*, 3224.
22. Krebs, M. P.; Holden, D. C.; Joshi, P.; Clark, C. L., III; Lee, A. H.; Kaushal, S. *J. Biol. Chem.* **2010**, *395*, 1063.
23. Li, T.; Sandberg, M. A.; Pawlyk, B. S.; Rosner, B.; Hayes, K. C.; Dryja, T. P.; Berson, E. L. *Proc. Natl. Acad. Sci.* **1998**, *95*, 11933.
24. Schöneberg, T.; Yum, J.; Wenkert, D.; Wess, J. *EMBO J.* **1996**, *15*, 1283.
25. Kagechika, H.; Kawachi, E.; Hashimoto, Y.; Himi, T.; Shudo, K. *J. Med. Chem.* **1988**, *31*, 2182.
26. Kagechika, H.; Kawachi, E.; Hashimoto, Y.; Shudo, K. *J. Med. Chem.* **1989**, *32*, 834.
27. Yamakawa, T.; Kagechika, H.; Kawachi, E.; Hashimoto, Y.; Shudo, K. *J. Med. Chem.* **1990**, *33*, 1430.
28. Hashimoto, Y. *Cell Struct. Funct.* **1991**, *16*, 113.
29. Nakamura, M.; Hamasaki, T.; Tokitou, M.; Baba, M.; Hashimoto, Y. *Bioorg. Med. Chem.* **2009**, *17*, 4740.
30. Dominguez, M.; Alvaez, R.; Perez, M.; Palczewski, K.; de Lera, A. R. *ChemBioChem* **2006**, *7*, 1815.
31. Imai, H.; Hirano, T.; Terakita, A.; Shichida, Y.; Muthyala, R. S.; Chen, R.-L.; Colmenares, L. U.; Liu, R. S. H. *Photochem. Photobiol.* **1999**, *70*, 111.
32. Kaneko, S.; Kagechika, H.; Kawachi, E.; Hashimoto, Y.; Shudo, K. *Med. Chem. Res.* **1991**, *1*, 220.
33. Renaud, J.-P.; Rochel, N.; Ruff, M.; Vivat, V.; Chambon, P.; Gronemeyer, H.; Moras, D. *Nature* **1995**, *378*, 681.
34. Bourguet, W.; Ruff, M.; Chambon, P.; Gronemeyer, H.; Moras, D. *Nature* **1995**, *375*, 377.
35. Okada, T.; Sugihara, M.; Bonder, A. N.; Elstner, M.; Entel, P.; Buss, V. *J. Mol. Biol.* **2004**, *342*, 571.
36. Palczewski, K.; Kumasaka, T.; Hori, T.; Behnke, C. A.; Motoshima, H.; Fox, B. A.; Le Trong, I.; Teller, D. C.; Okada, T.; Stenkamp, R. E.; Yamamoto, M.; Miyano, M. *Science* **2000**, *289*, 739.
37. Stojanovic, A.; Hwa, J. *Receptors Channels* **2002**, *8*, 33.